Nuclear Physics A385 (1982) 221–232

MULTILEVEL CALCULATIONS IN ODD-MASS NUCLEI (II). Positive-parity states

M.A. CUNNINGHAM*

A.W. Wright Nuclear Structure Laboratory, Yale University, New Haven CT 06511, USA

Received 8 March 1982

Abstract: We present the results of an analysis of the positive-parity states in the odd-mass transitional isotopes of xenon and barium, within the framework of the interacting boson-fermion model. These calculations include the four single-particle orbitals of the neutron 50–82 major shell: the $3s_{1/2}$, $2d_{3/2}$, $2d_{5/2}$ and $1g_{7/2}$ levels. We discuss the energy levels and electromagnetic properties of these states.

1. Introduction

This paper represents the second part of our discussion of multilevel calculations in odd-mass transitional nuclei. In the first part [1], which we shall refer to hereafter as I, we analyzed the negative-parity states in the odd-mass xenon and barium isotopes. These negative-parity states can be simply treated as originating from the coupling of a $1h_{11/2}$ neutron hole to the even-even core nucleus. However, as we saw in I, even for these presumably simple states, other fermion degrees of freedom were important in determining the properties of the low-lying structure. The $1h_{9/2}$ and $2f_{7/2}$ single-particle levels were crucial ingredients in the description of these states.

Thus the ability to perform calculations in which the odd nucleon can occupy more than one single-particle level is necessary even for the relatively simple cases of unique-parity states in these transitional nuclei. To describe the positive-parity states in the light xenon and barium isotopes will certainly require that all four positive-parity single-particle levels of the neutron 50–82 major shell be included in the calculations.

In sect. 2, then, we shall describe the energy spectra of these positive-parity states. The formalism for these calculations has been presented in I, so when necessary, we shall refer to the discussion there. In sect. 3, we discuss the electromagnetic properties of these states. This was a problem in the analysis of the negative-parity states, where detailed experimental information was not available, but in some instances this detailed information does exist for the positive-parity states. Thus it is possible to test in some detail the predictions of the model about the

* Current address: Schlumberger Well Services, P.O. Box 2175, Houston TX 77001.

mixing of the various fermion degrees of freedom. Some of this work has appeared in brief form previously [2]).

2. Energy spectra

The BCS formalism we established in I to handle the multilevel calculations was reliant on additional physical input to reduce the complexity of the overall calculations. The input required for these calculations was a set of single-particle energies, E_j, and the pairing gap energy, Δ. With these input data, the gap equations, (6) from I, can be solved for the quasi-particle energies, ε_j, and the occupation probabilities u_j and v_j. In this work, we attempted to extract the requisite single-particle energies from the experimental spectrum of ^{131}Sn [ref. [3])]. The pairing gap energy, Δ, was chosen to be $\Delta = 12A^{-1/2}$ MeV [ref. [4])].

In essence, this gives us six free parameters in the model: the interaction parameters A, Γ and Λ and the relative positions of the quasi-particle energies. (Since we do not compute an absolute binding energy, only three of the four quasi-particle energies are free parameters.) In table 1, we list the quasi-particle energies and occupation probabilities used in the calculations and in table 2, the boson-fermion interaction parameters.

2.1. ODD-MASS XENON ISOTOPES

The odd-mass xenon isotopes have been studied via a variety of experimental techniques, hence different aspects of the low-lying spectrum of each of the isotopes

TABLE 1

BCS parameters for the positive-parity state calculations (in units of MeV)

		$3s_{1/2}$	$2d_{3/2}$	$2d_{5/2}$	$1g_{7/2}$
^{123}Xe	ε_j	1.102	1.211	1.381	1.428
	v_j^2	0.405	0.276	0.858	0.817
^{125}Xe	ε_j	1.043	1.158	1.571	1.424
	v_j^2	0.494	0.346	0.886	0.855
^{127}Xe	ε_j	1.051	1.175	1.646	1.457
	v_j^2	0.587	0.432	0.908	0.885
^{129}Xe	ε_j	1.086	1.130	2.032	1.844
	v_j^2	0.683	0.539	0.927	0.910
^{131}Xe	ε_j	1.204	1.112	2.280	2.083
	v_j^2	0.779	0.667	0.944	0.932
^{129}Ba	ε_j	1.081	1.155	1.456	1.167
	v_j^2	0.587	0.432	0.908	0.885
^{131}Ba	ε_j	1.086	1.210	1.632	1.744
	v_j^2	0.683	0.539	0.927	0.910
^{133}Ba	ε_j	1.124	1.142	2.180	1.983
	v_j^2	0.779	0.667	0.944	0.932

TABLE 2

Hamiltonian parameters for the positive-parity state calculations (in units of MeV)

Isotope	A	Γ	Λ
^{123}Xe	−0.05	−0.10	0.60
^{125}Xe	−0.05	−0.10	0.60
^{127}Xe	−0.07	−0.10	0.60
^{129}Xe	−0.20	0.10	0.75
^{131}Xe	−0.25	−0.13	0.75
^{129}Ba	−0.10	−0.01	0.80
^{131}Ba	−0.15	−0.05	0.80
^{133}Ba	−0.30	−0.10	1.00

have been extracted. The isotope ^{123}Xe has been studied via decay measurements [5]), but the bulk of the information on the positive-parity states is derived from heavy ion, xn studies [6]). Consequently, what are observed experimentally are primarily the high-spin members of the various multiplets. In fig. 1, we show the observed spectrum and the results of our calculations. Not all of the computed levels are shown, because the level density is high enough to obscure the interesting features. As a rule, only those levels which correspond to the observed states have been plotted. The arrows connecting the states indicate the dominant decay modes.

The computed spectrum agrees quite well with the experimental one. The band heads are, of course, constrained to agree, but there is no major discrepancy among

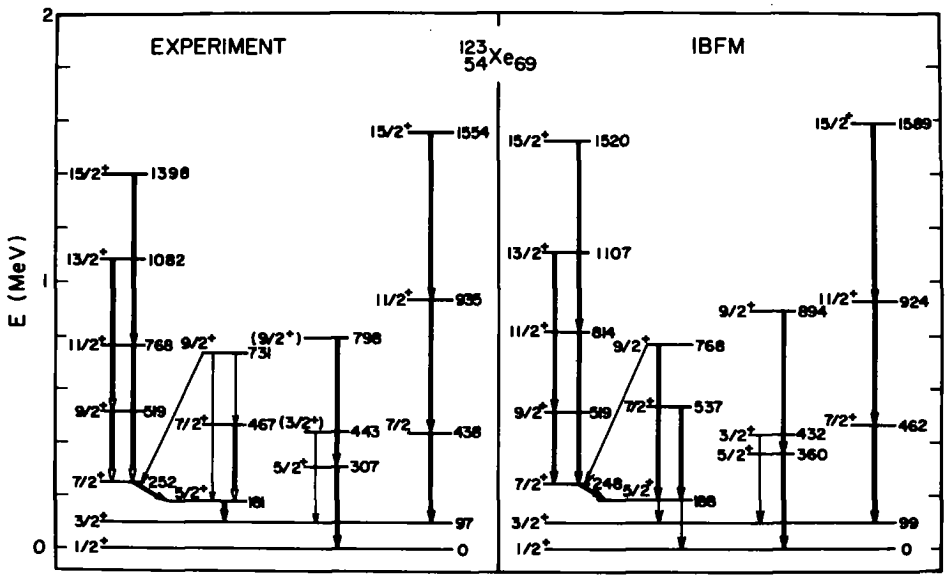

Fig. 1. Energy levels in ^{123}Xe. Experimental levels are from ref. [6]).

the remaining states. The $s_{1/2}$ band begins at the ground state and includes those states above the $\frac{5}{2}^+(307)$. The $d_{3/2}$ band begins at the $\frac{3}{2}^+(97)$ state and includes the $\frac{7}{2}^+(438)$, etc. Both of these bands have a $\Delta J = 2$ character, which arises from the particle nature of the $s_{1/2}$ and $d_{3/2}$ levels. The $g_{7/2}$ band, beginning at the $\frac{7}{2}^+(252)$ and the $d_{5/2}$ band, beginning at the $\frac{5}{2}^+(181)$ state both have $\Delta J = 1$, quasi-hole character. These characteristics are also reflected in the calculated spectrum. We shall leave a more detailed discussion of the electromagnetic properties to sect. 3, however.

The situation for the isotope ^{125}Xe is much the same. It has also been studied by the decay of Cs [5]), but again the primary source of information on these positive-parity states comes from heavy ion, xn studies [7]). The observed experimental spectrum is shown in fig. 2, along with the results of our calculations. There is good agreement between the experimental and theoretical spectra, which in fact, are quite similar to those of ^{123}Xe. The band spacing is slightly larger in ^{125}Xe, but this reflects the spacing of the levels in the even core nuclei: ^{124}Xe and ^{126}Xe. Notably, the parameter sets for the boson-fermion interaction are the same for these two isotopes. While this situation might be altered somewhat if other, low-spin

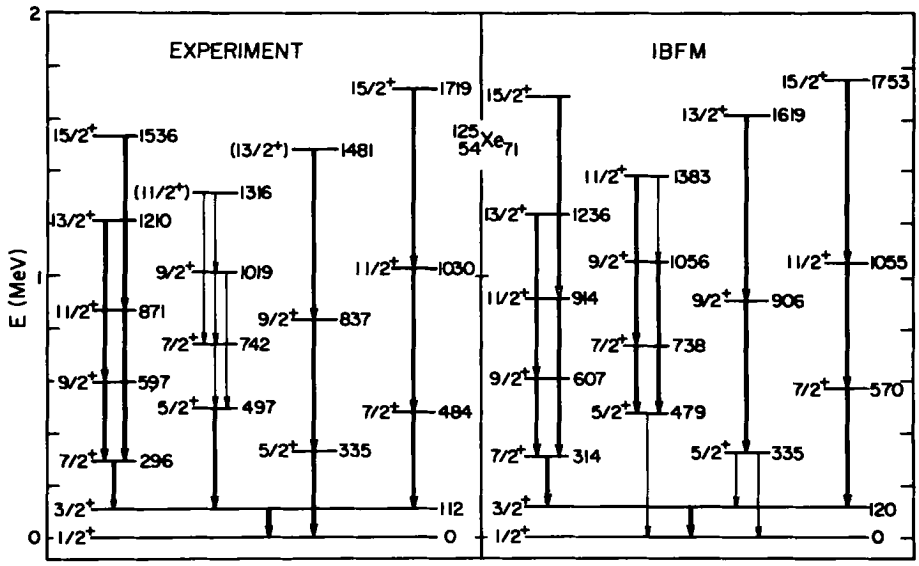

Fig. 2. Energy levels in ^{125}Xe. Experimental levels are from ref. [7]).

states are observed, it nonetheless indicates that the BCS formalism we have used has reasonable properties. Since the spectra of the two isotopes are similar, it would be surprising to find that the model parameters were substantially different.

The experimental information on ^{127}Xe also comes largely from heavy ion, xn studies [8]). The results of our calculations for this isotope are compared with the

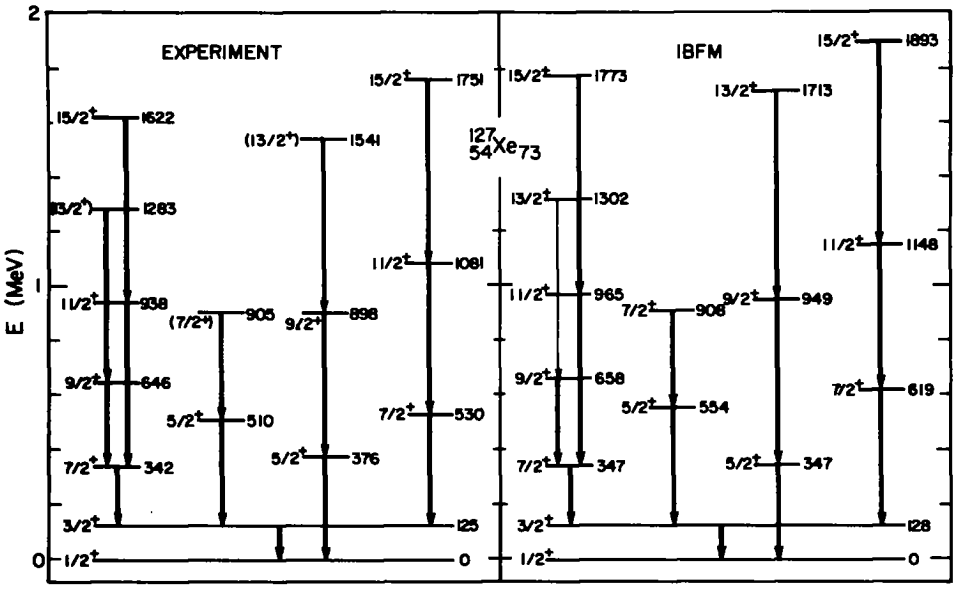

Fig. 3. Energy levels in ^{127}Xe. Experimental levels are from ref. [8]).

observed spectrum in fig. 3. The situation here resembles the two previous cases. The computed spectrum agrees quite well with the experimental one. Primarily the high-spin members of the multiplets are populated and these levels are reproduced with a parameter set only slightly different from those of the two lighter isotopes.

The situation is different for the isotope ^{129}Xe, however. Not only has this nucleus been studied via heavy ion, xn reactions [8–10]), but detailed decay studies exist as well [11]). Hence, many of the low-spin members of the various bands have been observed in addition to the high-spin states, which will provide much tighter constraints on the model parameters. In fig. 4, we show the high-spin part of the spectrum, as for the previous isotopes. The agreement between the computed and observed levels is quite good, which is the same situation as in the lighter isotopes. In fig. 5, we show the low-spin part of the experimental spectrum, along with the results of our calculations. Not all the calculated states have been plotted, since the level density gets rather high above 1 MeV. Hence, only the first few states of a given spin are shown. Overall, the agreement is rather impressive, but there are some discrepancies in detail. Experimentally, there is a $\frac{1}{2}^+$ state observed at 411 keV and a $\frac{3}{2}^+$ state at 589 keV. With the parameter set used in these calculations, the second $\frac{1}{2}^+$ state occurs at 528 keV and the third $\frac{3}{2}^+$ state at 409 keV.

This problem does not occur, however, in the calculated spectrum of ^{131}Xe, as seen at right in fig. 5. The experimental levels here are from refs. [8,9]). The $\frac{1}{22}^+$ state is observed at 565 keV and is calculated to be at 591 keV. The $\frac{3}{23}^+$ state is observed

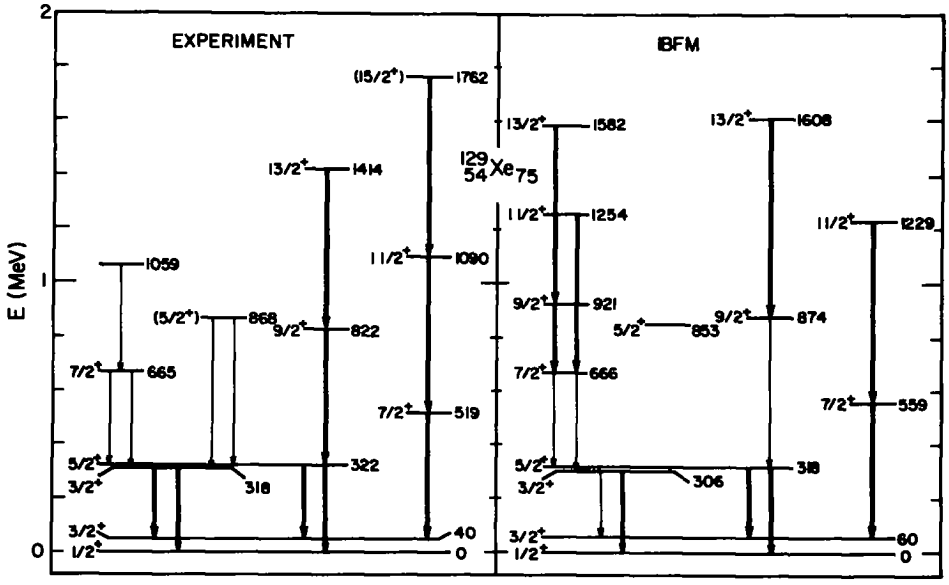

Fig. 4. Energy levels in ^{129}Xe. Experimental levels are from ref. [8]).

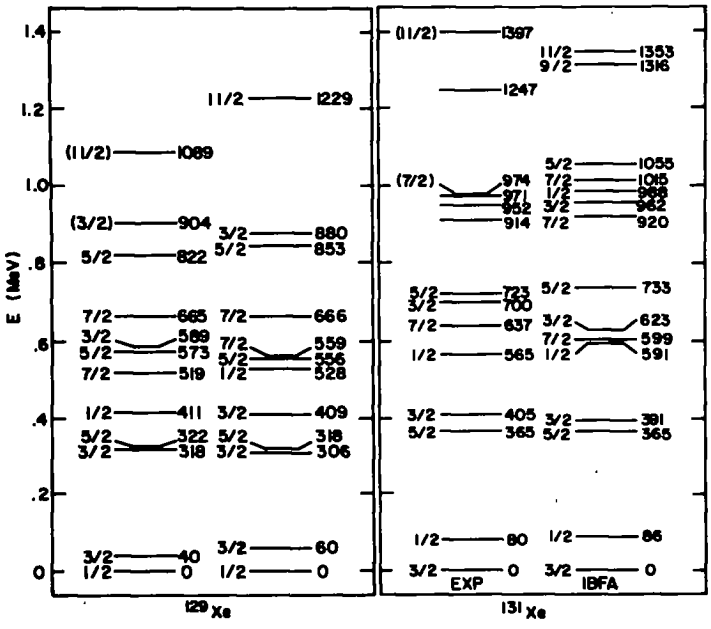

Fig. 5. Low-lying spectra of ^{129}Xe and ^{131}Xe. Experimental levels are from refs. [9–11]).

at 700 keV and is calculated to be at 623 keV. The difference between the agreement in the two isotopes is most likely due to different mixings of the single-particle degrees of freedom, but as this is not a weakly coupled system, it will be rather difficult to unravel the problem at this time. Hence, we shall defer our discussion of the situation to a later section in which we examine the electromagnetic properties of these states.

2.2. ODD-MASS BARIUM ISOTOPES

The spectra of the odd-mass barium isotopes are quite similar to those of the xenon isotopes we have just discussed. One of the most striking differences occurs in the isotope ^{129}Ba. In this nucleus, the $g_{7/2}$ level is observed [12,13]) to drop quite close, ~7 keV, to the ground state. In fig. 6, we compare the observed [12,13]) spectrum of ^{129}Ba, with the results of our calculations. The overall agreement is impressive, particularly in light of the fact that three single-particle levels lie within ~150 keV. Since this is a strongly coupled system, the observed agreement indicates that the mixing of the single-particle degrees of freedom is substantially correct.

The experimental spectra of ^{131}Ba and ^{133}Ba are also shown in fig. 6, along with our calculations for these two isotopes. The experimental levels are from refs. [14,15]). Again, the agreement between the observed and computed spectra is quite good.

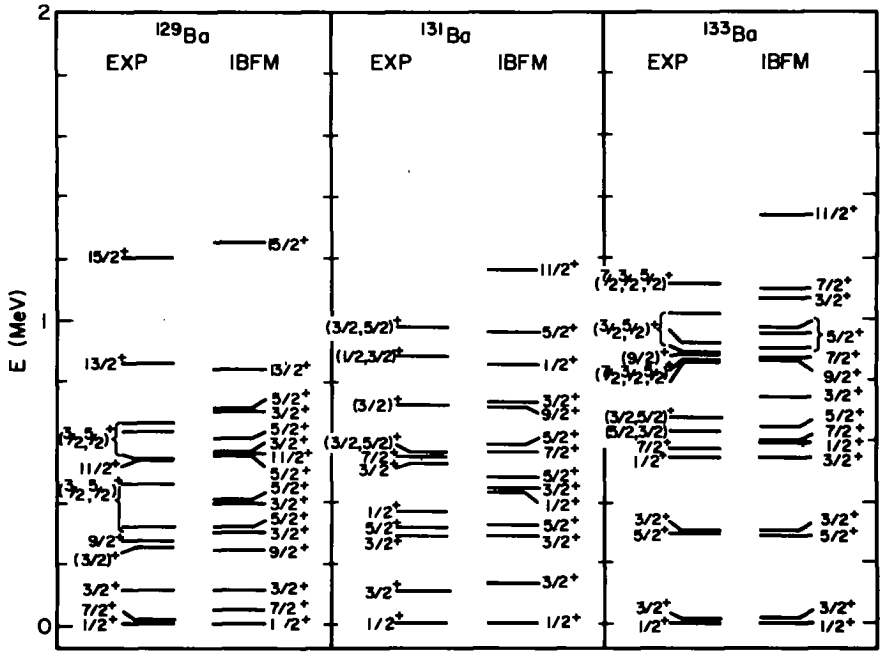

Fig. 6. Positive-parity states in $^{129-133}$Ba. Experimental data are from refs. [13-15]).

Notably, the $g_{7/2}$ level is much higher in these two isotopes than in ^{129}Ba. It appears at 544 keV in ^{131}Ba, and is presumably identified with the 577 keV state in ^{133}Ba. Our calculations certainly track the behavior of this state, but of course, cannot predict such precipitous behavior. It would be of considerable interest to complete the low-lying spectrum of these isotopes, ^{129}Ba in particular. Since in this isotope three single-particle states can be found within 150 keV of one another, the spectrum must be quite rich.

3. Electromagnetic properties

The isotopes ^{129}Xe and ^{131}Xe have been studied in particular detail [9–11]), so we shall focus our attention on these two isotopes in this report. We begin with an analysis of the E2 transitions.

3.1. E2 TRANSITIONS

The free parameters in the electric quadrupole operator are the boson and fermion effective charges, e_B and e_F. The boson charge, e_B, has been fixed [1]) by comparison with $B(E2:0^+ \rightarrow 2^+)$ values in the neighboring even-even isotopes to be $e_B = 0.13\ e \cdot b$. This value is used for all our calculations in the xenon and barium isotopes and is consistent with the values used in other systems [16,17]). The fermion effective charge, e_F, we have estimated from its single-particle value. Assuming that the radial matrix elements, $\langle r^2 \rangle$, are roughtly constant for levels in the same major shell, the effective charge becomes: $e_F = e_n \langle r^2 \rangle$. We have chosen the neutron effective charge to be $e_n = 0.5e$ and using the harmonic oscillator value for the radial matrix elements: $\langle r^2 \rangle = (N + \frac{3}{2})\hbar/M\omega$, we are led to a value of $e_F = -0.15e \cdot b$, where the sign arises from the hole-like nature of the odd neutron.

In table 3, we list the measured $B(E2)$ values in ^{129}Xe, along with the results of our calculations. For the most part, the theoretical values are in good agreement with the observed ones. This is quite remarkable in that nearly all transitions among the low-lying states have been observed. The situation for $B(E2)$ values in ^{131}Xe is much the same as for ^{129}Xe. Most of the transitions among the low-lying states have been observed, and agree quite well with the results of our calculations which we list in table 4.

The E2 transitions are, for the most part, dominated by the boson transitions, which represent the collective part of the problem. The single-particle aspects of the transitions become important where the boson matrix elements are small, such as for transitions between the band heads. In ^{129}Xe, these would be transitions involving the $\frac{1}{21}^+$, $\frac{3}{21}^+$, $\frac{5}{23}^+$ and $\frac{7}{22}^+$ states. For the most part, what transitions are observed among these levels are described reasonably well by the model, which indicates that the mixing of the various single-particle degrees of freedom is largely correct. There are, of course, some discrepancies. One such discrepancy can be

TABLE 3

Electromagnetic transitions in ^{129}Xe [refs. [9–11])]

Transition	B(E2) ($e^2 \cdot b^2$)		B(M1) ($10^{-3}\ \mu_N^2$)	
	exp	IBFM	exp	IBFM
$\frac{3}{21}^+ \rightarrow \frac{1}{21}^+$		0.011	49 (2)	0.1
$\frac{3}{22}^+ \rightarrow \frac{3}{21}^+$	$<5\times10^{-4}$	0.027	8 (1)	0.1
$\frac{3}{22}^+ \rightarrow \frac{1}{21}^+$	0.12 (1)	0.101	1.8 (2)	0.1
$\frac{5}{21}^+ \rightarrow \frac{3}{21}^+$	0.22 (3)	0.085	17 (3)	29.9
$\frac{5}{21}^+ \rightarrow \frac{1}{21}^+$	0.077 (7)	0.052		
$\frac{1}{22}^+ \rightarrow \frac{3}{22}^+$		0.024	12 (4)	4.6
$\frac{1}{22}^+ \rightarrow \frac{3}{21}^+$	0.044 (11)	0.080	4.5 (8)	0.2
$\frac{1}{22}^+ \rightarrow \frac{1}{21}^+$			4.5 (8)	1.1
$\frac{5}{22}^+ \rightarrow \frac{1}{21}^+$	0.057 (4)	0.067		
$\frac{3}{23}^+ \rightarrow \frac{1}{21}^+$	0.0032 (2)	0.011		0.1
$\frac{3}{24}^+ \rightarrow \frac{1}{21}^+$	0.0030 (2)	0.001		0.1

TABLE 4

Electromagnetic transitions in ^{131}Xe [refs. [9,10])]

Transition	B(E2) ($e^2 \cdot b^2$)		B(M1) ($10^{-3}\ \mu_N^2$)	
	exp	IBFM	exp	IBFM
$\frac{1}{21}^+ \rightarrow \frac{3}{21}^+$	0.0039 (5)	0.009		
$\frac{5}{21}^+ \rightarrow \frac{1}{21}^+$	0.030 (5)	0.028		
$\frac{5}{21}^+ \rightarrow \frac{3}{21}^+$	0.10 (1)	0.080	0.64 (12)	34.2
$\frac{3}{22}^+ \rightarrow \frac{3}{21}^+$	0.057 (4)	0.065	<7	0.1
$\frac{1}{22}^+ \rightarrow \frac{1}{21}^+$			>1	
$\frac{1}{22}^+ \rightarrow \frac{3}{21}^+$	0.048 (4)	0.070		0.2
$\frac{7}{21}^+ \rightarrow \frac{5}{21}^+$	0.005 (+0 −4)	0.003	2 (1)	10.2
$\frac{7}{21}^+ \rightarrow \frac{3}{21}^+$	0.081 (6)	0.092		
$\frac{3}{23}^+ \rightarrow \frac{3}{21}^+$	0.027 (2)	0.022		0.3
$\frac{5}{22}^+ \rightarrow \frac{3}{22}^+$	<0.031	0.006	58 (6)	35.2
$\frac{5}{22}^+ \rightarrow \frac{1}{21}^+$	0.068 (9)	0.071		
$\frac{5}{22}^+ \rightarrow \frac{3}{21}^+$	0.013 (1)	0.019	108 (8)	49.5
$\frac{7}{22}^+ \rightarrow \frac{3}{21}^+$	0.0050 (5)	0.0002		

found in the $\frac{5}{21}^+ \rightarrow \frac{3}{21}^+$ transition in ^{129}Xe. Here the mixing of the fermion configurations plays a more subtle role. The large observed B(E2) value for this transition is perhaps indicative that the $\frac{5}{21}^+$ state wave function is almost purely that of the $d_{3/2}$ coupled to the 2_1^+ configuration. Our calculations produce a model wave function that contains a large percentage of $s_{1/2}$ coupled to 2_1^+, which results in a smaller matrix element for the transition. This is a point that could possibly be examined more closely by particle-transfer experiments but, at this time, no such

work has been done. Nevertheless, the E2 transitions are in good order, and a more sensitive test of the mixing of the various single-particle levels can be found in the M1 transitions.

3.2. M1 TRANSITIONS

The free parameters in the M1 operator are the boson and fermion effective g-factors, g_B and g_F. The boson g-factor, g_B, we have fixed [1]) to be $g_B = 0.14\mu_N$, by comparison with magnetic moments of 2^+ states in the even–even xenon isotopes. For the xenon and barium isotopes we are discussing, the single-particle transitions are neutron transitions, which means that the fermion part of the total M1 operator, eq. (16) of I, simplifies considerably. The neutron orbital g-factor, g_{ln}, vanishes, and only the spin g-factor, g_{sn}, remains. The fermion effective g-factor, g_F, we have chosen to be $g_F = 0.6$, by comparison with the measured [12]) magnetic dipole moment of the $\frac{3}{21}^+$ state in ^{131}Xe. This value is consistent with that used for other nuclei in this mass region [3,7]), for quenching the spin g-factor.

The results of our calculations for B(M1) values in ^{129}Xe and ^{131}Xe are shown in tables 3 and 4, respectively, along with the experimental values. Since the M1 transitions are quite sensitive to the mixing of the various single-particle levels, it would not be too surprising to find rather large discrepancies in the B(M1) values. This is, in fact, what we find in tables 3 and 4. Only a few transitions agree to within a factor of three or four, and there are several which disagree by orders of magnitude. It is possible, at this point, to adjust the hamiltonian parameters and attempt to improve the agreement with the observed electromagnetic transitions, however, we shall not do so. Instead, we shall examine some of these transitions in detail, in the hope of illuminating the situation.

The $\frac{5}{21}^+ \rightarrow \frac{3}{21}^+$ transition is observed to be much weaker in ^{131}Xe than our calculations would indicate. The calculated E2 matrix element for this transition is slightly smaller than the observed one. If we take this to indicate that the model wave function for the $\frac{5}{21}^+$ state contains too large a percentage of $s_{1/2}$ configurations, then reducing this percentage would lead to a larger E2 matrix element. Additionally, such a step would lead to a smaller M1 matrix element. The reason for this is that a major component of the total M1 matrix element for this transition is given by the matrix element between the $(2_1^+ \times s_{1/2})^{(5/2)}$ and $(2_1^+ \times s_{1/2})^{(3/2)}$ configurations. Thus where the B(M1) values for this transition might indicate that the mixing of the fermion degrees of freedom is substantially in error, from our analysis, it is more likely that only a relatively small change in the model wave functions will bring the theoretical values into agreement with the observed ones.

The transition $\frac{3}{21}^+ \rightarrow \frac{1}{21}^+$ in ^{129}Xe is of particular interest since it will give us a great deal of information about the structure of these two states. If these two band heads are relatively pure, then the B(M1) value for the transition between them should be rather small. This is because the transition $d_{3/2} \rightarrow s_{1/2}$ is M1 forbidden. However,

this transition is observed to be rather large, which is indicative of a large percentage of $d_{3/2}$ configurations in the $\frac{1}{21}^+$ state. The $\frac{1}{21}^+$ state wave function produced by our calculations is built almost entirely from the $(0_1^+ \times s_{1/2})^{(1/2)}$ configuration, and the resulting M1 matrix element is small. Hence, the $\frac{1}{21}^+$ state must contain a significant percentage of $d_{3/2}$ configurations.

The point of this analysis should now be clear. While particular transition matrix elements may not agree as well as desired with the experimental values, it is possible to extract rather detailed information about the character of the state wave functions. This information could be then used as a further constraint on the model parameters and a new set of eigenfunctions could be generated. Even without such an elaborate analysis, however, the model provides a framework within which these collective states in transitional nuclei can be discussed.

4. Summary

The positive-parity states in the light isotopes of xenon and barium represent a rich area for study. Several single-particle levels play important roles in determining the low-lying structure in these nuclei, and the couplings are strong. Hence, some mechanism in which these several fermion degrees of freedom can be treated must be employed when trying to describe these states. In this report, we have presented the results of our analysis within the framework of the interacting boson–fermion model. The computed energy spectra are in substantial agreement with the observed ones, as are the electromagnetic properties of the states. It is clear that some refinements to the calculations will be required before a completely accurate description is in hand, but these will be small corrections to the mixing of the single-particle degrees of freedom. It is our belief that the formalism we have presented in this report will open the way for more, detailed calculations in odd-mass transitional nuclei.

The author would like to thank Professor Franco Iachello for many illuminating discussions, and Professors John Wood and Jolie Cizewski for their kind assistance with the experimental data. This work has been funded by USDOE Contract No. DE-AC02-76ER03074.

References

1) M.A. Cunningham, Nucl. Phys. **A385** (1982) 204
2) M.A. Cunningham, Phys. Lett., **106B** (1981) 11
3) C.M. Lederer and V.S. Shirley, ed., Table of Isotopes, 7th edition (Wiley, New York, 1977)
4) A. Bohr and B. Mottelson, Nuclear structure, vol. I (Benjamin, New York, 1969)
5) L. Westgaard, K. Aleklett, G. Nyman and E. Roekel, Z. Phys. **A275** (1975) 127
6) A. Luukko, J. Hattula, H. Helppi, O. Knuuttila and F. Donau, Nucl. Phys. **A357** (1981) 319
7) H. Helppi, J. Hattula and A. Luukko, Nucl. Phys. **A332** (1979) 183
8) H. Helppi, J. Hattula, A. Luukko, M. Jaaskelainen and F. Donau, Nucl. Phys. **A357** (1981) 333

9) D.C. Palmer, A.D. Irving, P.D. Forsyth, I. Hall, D.G.E. Martin and M.J. Maynard, J. of Phys. **G4** (1978) 1143
10) A.D. Irving, P.D. Forsyth, I. Hall and D.G.E. Martin, J. of Phys. **G5** (1979) 1595
11) G. Marest, R. Haroutunian, I. Berkes, M. Meyer, M. Rots, J. Deraedt, H. Van de Voorde, H. Oonis and R. Coussement, Phys. Rev. **C10** (1974) 402
12) J. Gizon, A. Gizon and J. Meyer-ter-Vehn, Nucl. Phys. **A277** (1977) 464
13) P. Brodeur, B.P. Pathak and S.K. Mark, Z. Phys. **A289** (1979) 289
14) A. Spalek, I. Rezanka, J. Frana, J. Jursik and M. Vobecky, Nucl. Phys. **A118** (1968) 161
15) D. von Ehrenstein, G.C. Morrison, J.A. Nolen, Jr. and N. Williams, Phys. Rev. **C1** (1970) 2066
16) G. Puddu, O. Scholten and T. Otsuka, Nucl. Phys. **A348** (1980) 109
17) P. von Isacker and G. Puddu, Nucl. Phys. **A348** (1980) 125